PHYSICAL REVIEW D **90,** 025019 (2014)

Semiclassical partition function for the double-well potential

D. Kroff,[1,2,*] A. Bessa,[3,†] C. A. A. de Carvalho,[1,‡] E. S. Fraga,[1,4,5,§] and S. E. Jorás[1,‖]

[1]*Instituto de Física, Universidade Federal do Rio de Janeiro, Caixa Postal 68528, 21941-972 Rio de Janeiro, Rio de Janeiro, Brazil*

[2]*Institute de Physique Théorique CEA/DSM/Saclay, Orme des Merisiers 91191 Gif-sur-Yvette cedex, France*

[3]*Escola de Ciências e Tecnologia, Universidade Federal do Rio Grande do Norte, Caixa Postal 1524, 59072-970 Natal, Rio Grande do Norte, Brazil*

[4]*Institute for Theoretical Physics, J. W. Goethe-University, D-60438 Frankfurt am Main, Germany*

[5]*Frankfurt Institute for Advanced Studies, J. W. Goethe University, D-60438 Frankfurt am Main, Germany*

(Received 19 November 2013; published 15 July 2014)

We compute the partition function and specific heat for a quantum-mechanical particle under the influence of a quartic double-well potential nonperturbatively, using the semiclassical method. Near the region of bounded motion in the inverted potential, the usual quadratic approximation fails due to the existence of multiple classical solutions and caustics. Using the tools of catastrophe theory, we identify the relevant classical solutions, showing that at most two have to be considered. This corresponds to the first step towards the study of spontaneous symmetry breaking and thermal phase transitions in the nonperturbative framework of the boundary effective theory.

DOI: 10.1103/PhysRevD.90.025019 PACS numbers: 03.65.Sq, 05.30.-d, 11.10.Wx

I. INTRODUCTION AND MOTIVATION

In the analytic description of phase transitions in particle physics and nuclear theory, one usually relies on the effective model approach, given the complexity of the fundamental theories involved. If we consider strong interactions, the phase diagram related to chiral symmetry restoration and deconfinement is a particularly interesting example, since they are within experimental reach and currently being investigated by different experiments at RHIC-BNL and LHC-CERN [1]. Usually, one generally adopts low-energy effective models such as the linear sigma model [2,3] and the Nambu–Jona-Lasinio model [4], which can be combined with different versions of the Polyakov loop model [5]. The standard approach, then, corresponds to the computation of a thermal effective potential from which one can extract information on the different phases and all thermodynamic quantities, so that one can build a phase diagram.

In most cases, the computation is performed in the mean-field approximation with one-loop thermal corrections assuming homogeneous and static background fields [6]. Frequently, vacuum loop contributions are ignored, even in a theory with spontaneous symmetry breaking, where the presence of a condensate always modifies the masses, which then become medium-dependent quantities, affecting significantly the phase structure [7–16]. So, the highly nonlinear behavior of the effective potential for large fields is completely missed, as well as nonperturbative effects (with the exception of the treatment within the functional renormalization group [17]). Those aspects can, in principle, dramatically modify the phase structure provided by a given effective model.

The boundary effective theory formalism [18,19] furnishes a nonperturbative method to calculate the partition function of quantum systems in thermal equilibrium in which configurations that are not strictly periodic play the main role. In such approach, one can compute the thermal one-loop effective potential for a system of massless scalar fields with quartic interaction [20]. The calculation relies on the solution of the classical equation of motion for the field, and Gaussian fluctuations around it. The result is nonperturbative and differs from the standard one-loop effective potential [21] for field values larger than $T/\sqrt{\lambda}$, T being the temperature and λ the coupling [20].

The natural extension would be the calculation of the effective potential in the case with spontaneous symmetry breaking. That would allow for the description of phase transitions in effective models incorporating nonlinear and nonperturbative effects, as well as controlling the infrared divergences of thermal field theory in a well-defined and relatively simple way [18,19,22]. However, to develop the method to be applied in this case, it is necessary to deal with multiple classical solutions, since more than one solution may satisfy the boundary conditions in Euclidean time.

As a first step towards the study of spontaneous symmetry breaking and thermal phase transitions using

*kroff@if.ufrj.br
†abessa@ect.ufrn.br
‡aragao@if.ufrj.br
§fraga@if.ufrj.br
‖joras@if.ufrj.br

 © 2014 American Physical Society

the boundary effective theory, in this paper we focus on the simpler case of computing the semiclassical partition function for a quartic double-well potential in quantum statistical mechanics. Although apparently trivial and straightforward, the inverted potential in this case has a region of bounded motion. Therefore, one also has to deal with multiple solutions and their coalescence as the temperature changes. The usual quadratic approximation may yield good results when such solutions are far away from each other in functional space, but, as we shall see later on, this is not so in the opposite scenario. Among the numerous solutions, we use the framework of catastrophe theory to identify the only two relevant ones, following Refs. [23,24]. We then compute the partition function and specific heat, obtaining the correct limits at both high and low temperatures, and a regular behavior where the usual quadratic approximation diverges.

This problem—the existence of multiple classical solutions—has been tackled by a few papers, all of them interested in the calculation of the propagator (where the Morse index does play an important role): In Ref. [25], the author studies an spherically symmetric potential which also yields caustics, but the paper aimed at calculating the energy levels of the system. Reference [26] was also interested in the energy levels and in particular its ground-state value. There, the authors use complex-valued trajectories and actions and take into account an infinite number of periodic solutions—as we shall see later on, we show that one shall use only two real ones, that are strictly stable. Reference [27] does go beyond quadratic order, like we do, but goes up to third order, since that is enough to yield a well-behaved Airy solution, which is nicely interpreted as an evanescent wave. Reference [28] also studies the double well and mentions that one can get rid of the singularities going to fourth order, but the paper focuses on the low-temperature (large-β) limit—the dilute instanton gas approximation—as opposed to us, who make no such restriction on the range of the temperature. The authors do mention the negative-eigenvalue solutions but we show that they should not be taken into account. None of those papers calculate the specific heat and its behavior at both small and large temperature.

The paper is organized as follows. In Sec. II we review general characteristics of the semiclassical path-integral representation of the partition function and discuss the case of multiple solutions in the double well. In Sec. III we use the tools from catastrophe theory to deal with the coalescence of solutions and identification of relevant minima. In Sec. IV we present results for the partition function and the specific heat, discussing their controlled behavior and the domain of validity of our approximation. Section V contains our summary. Elements and some technical details of catastrophe theory are presented in the Appendices.

II. SEMICLASSICAL PATH-INTEGRAL REPRESENTATION OF THE PARTITION FUNCTION

A. General features

In statistical mechanics, the partition function for a system in contact with a thermal reservoir at temperature T is given by the sum of a probabilistic weight, the diagonal elements of the density matrix, over a stochastic variable that labels the state of the system. This object is of fundamental importance, as it encodes all the thermodynamic information.

For a one-dimensional quantum-mechanical system consisting of a single particle, the stochastic variable can be chosen as the Schrödinger-picture position operator eigenvalue. Therefore, if the dynamics is dictated by the Hamiltonian operator $\hat{H}$, the partition function is written as $(1/\beta \equiv k_B T)$

$$Z = \int_{-\infty}^{\infty} dx_0 \langle x_0 | \exp(-\beta \hat{H}) | x_0 \rangle. \tag{1}$$

The matrix element in the previous equation can be understood as the analytic continuation of the transition amplitude $\langle x_0 | \exp[-i(\hat{H}/\hbar)(t-t')] | x_0 \rangle$ to imaginary time, allowing for a formal expression for the diagonal elements of the density matrix in terms of path integrals [29]. If we restrict our analysis to systems subject to velocity-independent potentials, the desired expression has the well-known form:

$$\langle x_0 | \exp(-\beta \hat{H}) | x_0 \rangle = \int_{x(0)=x(\beta\hbar)=x_0} [\mathcal{D}x(\tau)] e^{-S_E/\hbar}, \tag{2}$$

where

$$S_E[x] = \int_0^{\beta} d\tau \left[\frac{m}{2} \left(\frac{dx}{d\tau} \right)^2 + V(x) \right]. \tag{3}$$

In other words, the diagonal elements of the density matrix are obtained integrating the exponential of the Euclidean action S_E over the paths $x(\tau)$ in imaginary time satisfying the conditions $x(0) = x(\beta\hbar) = x_0$.

For convenience we define the dimensionless quantities $q \equiv x/x_N$, $\theta \equiv \omega_N \tau$, $\Theta \equiv \beta\hbar\omega_N$, $U(q) \equiv V(x_N q)/m\omega_N^2 x_N^2$ and $g \equiv \hbar/m\omega_N x_N^2$ where ω_N^{-1} and x_N are the natural time and length scales of the problem under consideration, respectively. In terms of these, the partition function can be written as follows:

$$Z(\Theta) = \int_{-\infty}^{\infty} dq_0 \int_{q(0)=q(\Theta)=q_0} [\mathcal{D}q(\theta)] e^{-I/g}, \tag{4}$$

where

$$I[q] = \int_0^\Theta d\theta \left[\frac{1}{2}\left(\frac{dq}{d\theta}\right)^2 + U(q)\right]. \quad (5)$$

In general, it is not possible to solve exactly the path integral above, but we can still resort to approximation procedures in order to evaluate it. A very natural approach is the Jeffreys-Wentzel-Kramers-Brillouin (JWKB) [30] asymptotic expansion in $\hbar$ (or g)—also known as semiclassical approximation—that we briefly discuss below.

The trajectories that extremize the Euclidean action $I[q]$ are those satisfying the Euler-Lagrange equation ($U' \equiv dU/dq$),

$$\frac{d^2 q_c}{d\theta^2} - U'(q_c) = 0, \quad (6)$$

subject to the boundary conditions $q(0) = q(\Theta) = q_0$. In other words, these are the classical solutions describing the motion of a particle under the influence of the inverted potential $-U(q)$.

Due to its Euclidean nature, the path integral in Eq. (2) is dominated by the functions in the vicinity of those that *minimize* $I[q]$. So, one has to determine among the solutions of (6) those representing minima, which we denote by $\bar{q}_c{}^i$. Expanding the action around the minima, we have $I[\bar{q}_c{}^i + \eta] = I[\bar{q}_c{}^i] + I_2[\bar{q}_c{}^i, \eta] + \delta I[\bar{q}_c{}^i, \eta]$, where

$$I_2[\bar{q}_c{}^i, \eta] = \frac{1}{2}\int_0^\Theta d\theta \eta(\theta)\left[-\frac{d^2}{d\theta^2} + U''(\bar{q}_c{}^i)\right]\eta(\theta), \quad (7)$$

$$\delta I[\bar{q}_c{}^i, \eta] = \sum_{k=3}^{\infty}\frac{1}{k!}\int_0^\Theta d\theta U^{(k)}(\bar{q}_c{}^i)\eta^k(\theta). \quad (8)$$

Keeping only terms up to quadratic order in the fluctuations, one obtains the so-called *standard* semiclassical approximation for the partition function:

$$Z \approx \int_{-\infty}^{\infty} dq_0 \sum_i \exp(-I[\bar{q}_c{}^i]/g)\Delta^{-1/2}, \quad (9)$$

where Δ is the determinant of the quadratic fluctuation operator

$$\Delta = \det \hat{F}[\bar{q}_c{}^i] = \det\left[-\frac{d^2}{d\theta^2} + U''(\bar{q}_c{}^i)\right]. \quad (10)$$

As an example, let us consider a single-well potential $U(q)$, whose global minimum is located at the point q_m, as depicted in Fig. 1. Following the method described above, one has to obtain the solutions describing the classical motion of the particle under the influence of the inverted potential that leaves the point q_0 at $\theta = 0$ and returns after a time interval Θ.

As the potential $-U(q)$ is unbounded from below, if the particle departs from a point such that $q_0 < q_m$ ($q_0 > q_m$), it will only return to the initial position if its initial velocity points to the right (left), otherwise the particle will move directly towards $-\infty$ ($+\infty$). However, the initial velocity cannot be arbitrarily large, for if the particle energy is greater than the height of the potential barrier, it will not return to its initial position either, as it will move directly towards $+\infty$ ($-\infty$). Thus, the maximum possible value for the particle energy is exactly the barrier height.

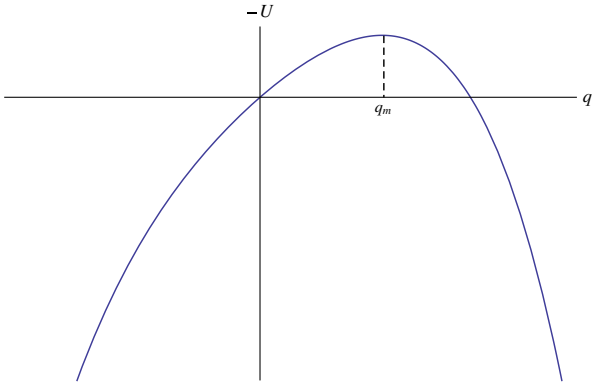

FIG. 1 (color online). Single-well inverted potential.

For a fixed value of q_0, the time the particle spends going from the initial position up to the turning point q_t is a function of q_t only, given by the following expression:

$$\frac{\Theta}{2} = \mathrm{sign}(q_t - q_0)\int_{q_0}^{q_t}\frac{dq}{\sqrt{2[U(q) - U(q_t)]}}. \quad (11)$$

Clearly, the previous expression vanishes when $q_t = q_0$. But, as the turning point moves further up the barrier, the time of flight increases continuously, diverging when q_t is exactly at the top. Therefore, for any value of Θ, it is possible to determine *the one solution* satisfying $q(0) = q(\Theta) = q_0$ by choosing the appropriate turning point. It is, then, a straightforward task to implement the semiclassical method, as was demonstrated in detail in Ref. [31]. In fact, even the D-dimensional case can be treated for central potentials [32].

B. Double-well potential: Multiple solutions

The problem becomes more intricate in the case of double-well potentials. Suppose now that $U(q)$ represents a double-well potential with degenerate minima located at $q = a$ and $q = b$, with $a < b$, e.g. like the one sketched in Fig. 2. As we shall see, it is now necessary to deal with multiple classical solutions.[1]

If $q_0 < a$ or $q_0 > b$, the particle lies in a region of unbounded motion under the potential $-U$, resembling the

[1]The quartic double-well potential at finite temperature has been investigated previously using semiclassical, variational and perturbative methods, e.g. in Refs. [28,33–35].

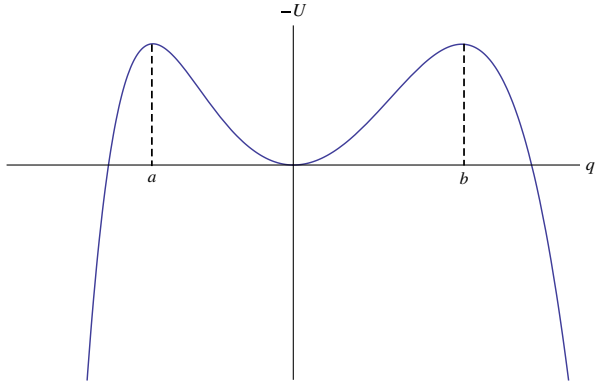

FIG. 2 (color online). Double-well inverted potential.

single-well case.[2] It is trivial to extend the arguments given in the previous section and conclude that, as before, each pair (q_0, Θ) defines a unique solution to Eq. (6).

Let us now analyze what happens when $a < q_0 < b$, i.e. when the particle starts in the well of $-U(q)$. Once again, its energy has to be smaller than the barrier height, otherwise the particle will leave the well towards $\pm\infty$ without ever returning to its initial position. In other words, there is a maximum allowed speed for such particles and all the solutions departing from a point in the well must always remain therein. In this region of bounded motion, we see a much richer structure, with the possibility of multiple classical solutions for a given q_0, depending on Θ.

If the temperature is high enough, the available time of flight is still very restrictive. Accordingly, since the speed is limited, the particle will be able to move only towards the nearest peak (q_t and q_0 will have the same signal—see Fig. 3, lower panel), but it will not be able to reach points too far from its initial position. Thus, in this limit, we still have a single solution for every q_0. Lowering the temperature (increasing Θ), the particle will be able to go further away and eventually it will be able to reach also the opposite side of the potential well and return to its initial position. From then on (i.e, for lower temperatures), a fixed q_0 will no longer define a unique classical solution [23].

In order to apply the semiclassical method with multiple solutions, one has to be able to identify and keep only those representing minima of the Euclidean action in functional space, discarding maxima and saddle points, which both correspond to unstable solutions with at least one negative eigenvalue[3] of the quadratic fluctuation operator $\hat{F}[q_c]$, defined in Eq. (10).

[2]It is essential for this piece of the argument that the maxima of the inverted potential are degenerate. The method discussed in the present work can be generalized and applied to the case of nondegenerate minima.

[3]The solution $q_c(\theta)$ is a minimum when all the eigenvalues are positive, a maximum when they are all negative and a saddle point otherwise.

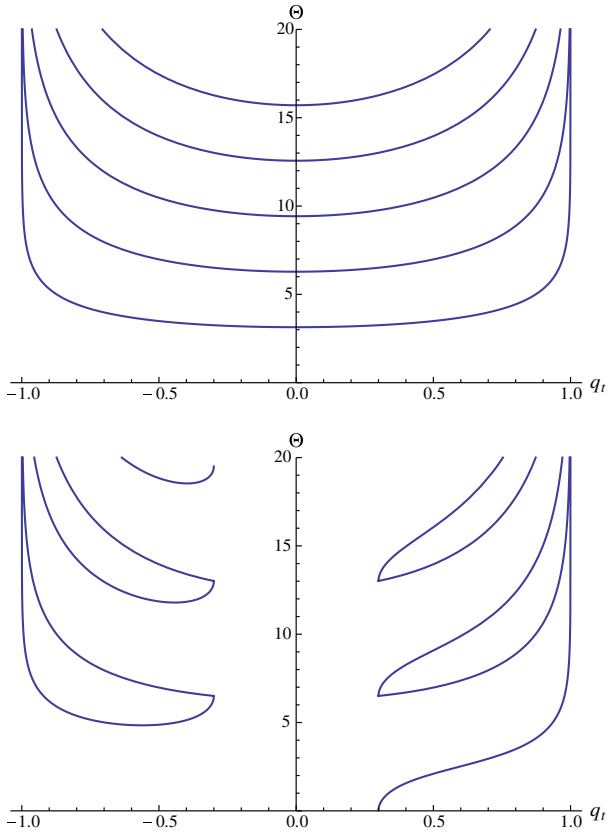

FIG. 3 (color online). Plots of the time of flight Θ vs. the turning point q_t for $q_0 = 0$ (upper) and $q_0 = 0.3$ (lower). In the upper panel, the trivial solution $q_0 = q_t = 0 = q(t)\forall t$, although valid for all Θ, is not shown.

In the next section, we restrict ourselves to a quartic double-well potential and, using the language of catastrophe theory, we not only identify how the number of solutions changes as we vary the parameters (q_0, Θ), but also find a straightforward criterium to determine which classical trajectories must be taken into account.

III. COALESCENCE OF SOLUTIONS

A. Caustics and catastrophes for the quartic double-well potential

From now on, we consider the specific case of a quartic double-well potential, $V(x) = -m\omega^2 x^2/2 + \lambda x^4/4$. Writing it in terms of $q \equiv x/x_N$, $x_N \equiv \sqrt{m\omega^2/\lambda}$:

$$U(q) = \frac{\lambda}{m^2\omega^4} V(x_N q) = -\frac{1}{2}q^2 + \frac{1}{4}q^4. \qquad (12)$$

As discussed previously, if the temperature is sufficiently high, there is only one closed path, with a single turning point, for every q_0. Lowering the temperature, we go from a single-solution to a three-solution regime. Lowering it even further, we reach a five-solution regime and so on [23].

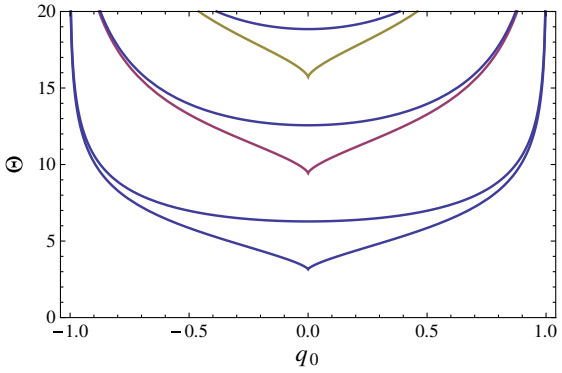

FIG. 4 (color online). The plane (q_0, Θ) is divided into regions with different number of classical solutions. The frontiers between those regions, named caustics, are shown above. The smooth curves indicate the coalescence of strictly periodic solutions, i.e, those that begin and end at the same position and at the same velocity.

Figure 3 is a clear illustration of the feature of solution bifurcation. It shows the plots of the time of flight Θ vs. the first turning point q_t of the classical path for two different values of q_0. One can read directly from the plots the values of q_t that allow the particle to return to q_0 in a time interval Θ. As fixing the initial position and the first turning point defines univocally the classical trajectory, the plot shows the number of classical solutions related with each value of the time of flight.

Thus, the plane (q_0, Θ) is divided into several regions with different numbers of solutions, as shown in Fig. 4. Moving from a certain region to a neighboring one, two solutions are either created or annihilated. Exactly at the frontier between those regions, two classical trajectories coalesce. The curves defining the frontiers between two such regions are named *caustics*, for they are analogous to the optical phenomenon. In our case, the classical solutions play the role of the light rays and the action replaces the optical distance [23].

The information depicted in Figs. 3 and 4 is combined into a single 3D plot in Fig. 5.

To apply the semiclassical method to compute the partition function for the double-well potential we must determine which of the solutions are actual minima of the action and track them down. To do so, we use the framework of catastrophe theory [36], which classifies and studies how the extrema of certain functions coalesce and emerge. A brief summary of a few ingredients of catastrophe theory is presented in Appendix A.

B. Finding the minima

Following Appendix A, new real solutions of (6), i.e. new extrema of the Euclidean action, emerge whenever the fluctuation determinant Δ vanishes. This provides a criterium to determine the location of the caustics.

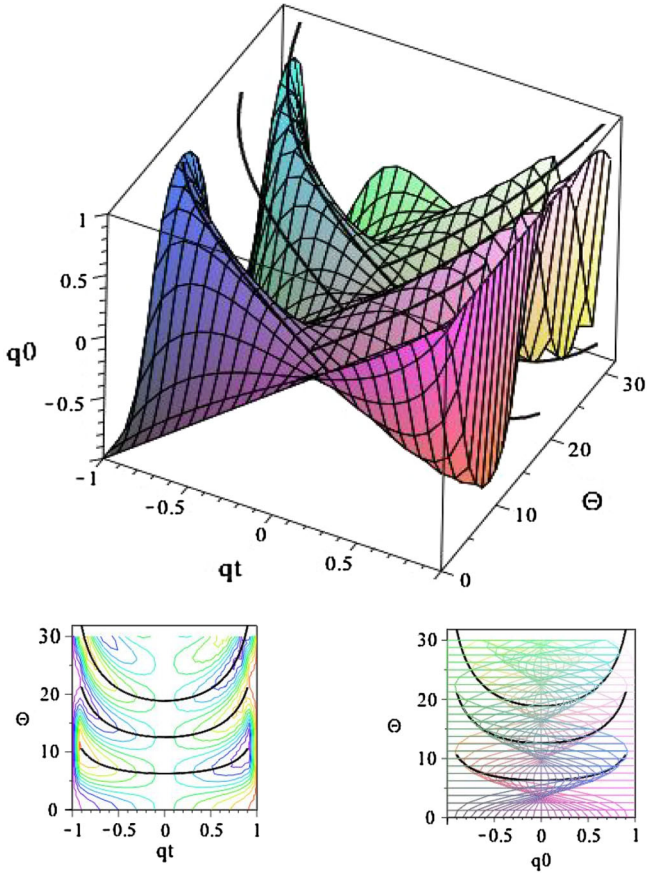

FIG. 5 (color online). Three-dimensional plot of $q_t \times q_0 \times \Theta$ (upper panel) and its projections onto the planes $q_t \times \Theta$ (bottom left) and $q_0 \times \Theta$ (bottom right).

It is clear that, for the problem under consideration, there are only two variables controlling the pattern of action extrema, which we choose to be q_0 and Θ.[4] Therefore, we are dealing with catastrophes whose codimension is not greater than two. The only two catastrophes satisfying this condition are the fold and the cusp, both having only one essential variable or coordinate [36]. In other words, we know that, in our case, only one eigenvalue of the fluctuation operator vanishes when a caustic is crossed.

Therefore, we can focus on one direction of the functional space: the one defined by the eigenfunction whose lowest eigenvalue vanishes. If we project the action onto that direction and perform a change of variables (see Appendix B), we will reach the so-called *normal form* (see Table I):

$$I_N(z) = \frac{1}{4}z^4 + \frac{u}{2}z^2 + vz + s, \tag{13}$$

where z is the coordinate associated to the aforementioned direction in functional space and u and v are the control parameters. The bifurcation set is then given by

[4]The third available quantity, q_t, can be written in terms of the chosen ones.

TABLE I. The five simplest elementary catastrophes, their codimension (number of control parameters), dimensions (number of coordinates) and the normal forms of their generating functions.

Catastrophe	Codimensions	Dimensions	Normal form
Foldl	1	1	$x^3/3 + ux$
Cusp	2	1	$x^4/4 + ux^2/2 + vx$
Swallowtail	3	1	$x^5/5 + ux^3/3 + vx^2/2 + wx$
Elliptic umbilic	3	2	$x^3 - 3xy^2 - u(x^2 + y^2) - vx - wx$
Hyperbolic umbilic	3	2	$x^3 + y^3 + uxy - vx - wy$

$$\frac{dI_N}{dz} = \frac{d^2 I_N}{dz^2} = 0 \Rightarrow 27v^2 + 4u^3 = 0. \qquad (14)$$

The previous equation defines a cusp in the control parameter space (u, v), dividing it in two parts—see Fig. 6. To the right of the curve the action has one minimum, to its left there are one maximum and two minima.

If the cusp is crossed at its vertex, as in arrow 1 of Fig. 6, the original minimum becomes a maximum and two symmetric minima appear—see Fig. 7. On the other hand, if the crossing happens at any other point, as in arrow 2 in Fig. 6, the original minimum remains and two new solutions appear—a maximum and a new (local) minimum—see Fig. 8. In the former case, one solution splits into three; in the later, two new solutions emerge (out of the coalescence of their complex counterparts—see next paragraph) while the previously existing minimum is unaffected. This picture agrees with our previous statement that the number of solutions of (6) increases by two.

It is useful to think of exactly the same merging of extrema that happens in the algebraic equation (13). Being a fourth-order polynomial with real coefficients, there are always three extrema which may be either real or imaginary, depending on the values taken by the control parameters $\{u, v\}$. Then, one usually speaks of the coalescence of *complex* solutions (which always come in pairs and are conjugate to each other) and their subsequent separation along the real axis, as opposed to their plain *creation* out of nothing.

Previous works (see, for instance, Ref. [26]) took into account such complex-valued trajectories. In Fig. 9 we plot the level curves of the imaginary part of the action (13), which define the steepest descent path crossing the only classical solution before the first caustic takes place (first panel). Even as u changes and the caustic is crossed, the real axis is always the steepest path crossing the former only extremum.

As one lowers the temperature, at the next catastrophe the classical trajectory with highest action is the one that gives rise to two new solutions. So, the solutions emerging after the second caustic are still maxima along the direction (in functional space) of the first catastrophe. On all the forthcoming catastrophes, the same happens: new solutions originate from the one with the highest action. Thus, in the multiple-solution regime, the only solutions that are actual minima of the action are those that are minima along the direction of the first catastrophe. So, to apply the semiclassical method, we just have to be concerned about at most two classical solutions.

Moreover, as the first catastrophe happens before the emergence of strictly periodic solutions (in fact, these solutions appear only in the second catastrophe), we can guarantee that the solutions we have to keep have a single

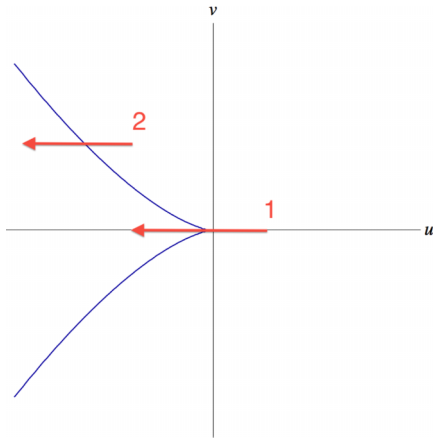

FIG. 6 (color online). Cuspid $27v^2 + 4u^3 = 0$ in the control parameter space. See text and Figs. 7 and 8 for explanation of the arrows.

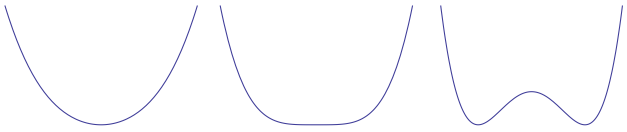

FIG. 7 (color online). Behavior of the action in functional space when the cusp is crossed at the vertex. See arrow 1 in Fig. 6.

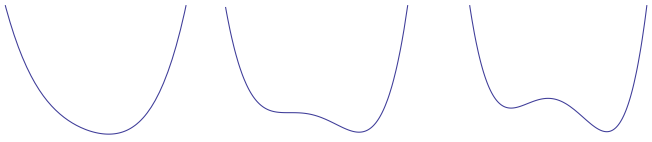

FIG. 8 (color online). Behavior of the action in functional space when the cusp is crossed at a point that is not the vertex. See arrow 2 in Fig. 6.

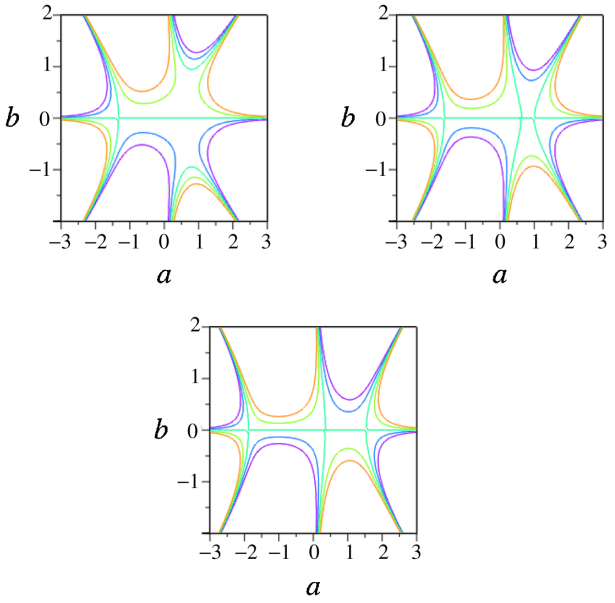

FIG. 9 (color online). Level urves of the imaginary part of the action (13), where $a \equiv \mathcal{R}(z)$ (horizontal axis), $b \equiv \mathcal{I}(z)$ (vertical axis). We adopted $v = 1$ and $u = -1, -2, -3$, for the first, second and third panels, respectively, i.e, following arrow 2 in Fig. 6.

turning point. Hence, there is a criterium that allows us to determine which solutions of (6) we must use when applying the semiclassical method: *at the end we need only the single-turning-point trajectories*.

IV. PARTITION FUNCTION AND SPECIFIC HEAT FOR THE DOUBLE-WELL POTENTIAL

The solutions of the classical equation of motion for the potential given in Eq. (12) can be expressed in terms of Jacobi elliptic functions [37,38]. In particular, the solutions we are interested in, the ones with a single turning point, can be written as

$$q(\theta) = q_t \mathrm{cd}[\sqrt{1 - q_t^2/2}(\theta - \Theta/2), k] \qquad (15)$$

where we define $k \equiv q_t/\sqrt{2 - q_t^2}$. In Fig. 10 we show plots of the classical solutions before and after the first caustic.

For those trajectories, the fluctuation determinant Δ defined in (10) can be expressed as [23,31]:

$$\Delta = \frac{4\pi g[U(q_t) - U(q_0)]}{U'(q_t)} \left(\frac{\partial \Theta}{\partial q_t}\right)_{q_0} \qquad (16)$$

That being so, we can now use the previous equation in (9) to obtain the semiclassical partition function.

The standard semiclassical method yields a very good approximation for the density matrix before and after the first caustic. However, as discussed in Ref. [24] (see also below), the method breaks down at the caustic, since, there, by construction, the determinant Δ vanishes—see Eq. (9). This can be easily understood in the functional space

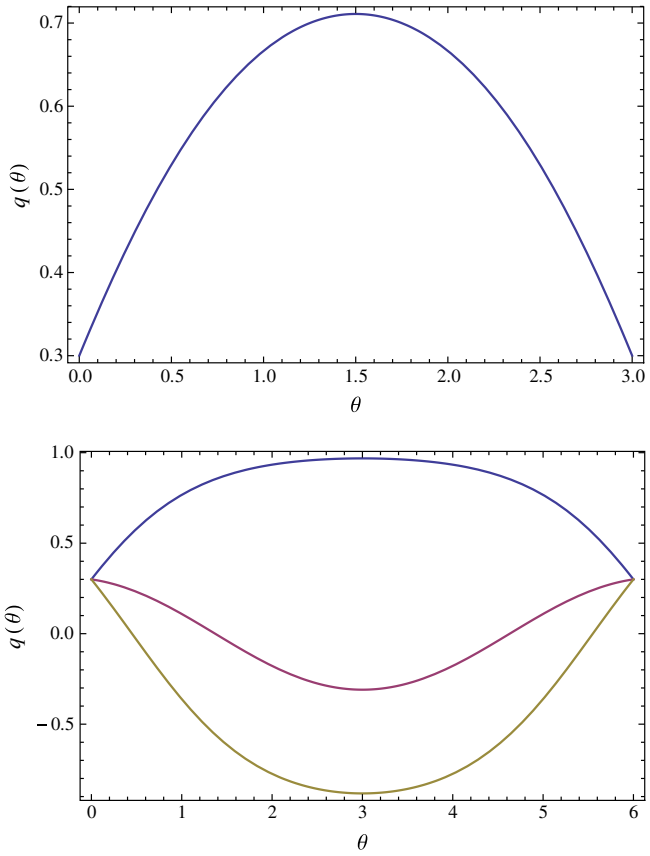

FIG. 10 (color online). Plots of the classical solutions $q(\theta)$ for $q_0 = 0.3$ and $\Theta = 3$ (upper), before the first caustic, and for $\Theta = 6$ (lower), after the first caustic. In the latter, the middle curve corresponds to a (local) maximum of the action and, thus, will not be taken into consideration in the subsequent calculation of the partition function.

(see Figs. 7 and 8): the second derivative of the action vanishes whenever two (or three) solutions coalesce. Therefore, any approximation that stops at the quadratic term is bound to diverge at this point.

This singularity, however, is integrable (as also noted in [24]). This statement can be proved if we perform a change of variables in (9) from q_0 to q_t. Using (11) and (16) we can write, following Ref. [31],

$$\left(\frac{\partial q_0}{\partial q_t}\right)_{\Theta} = -\frac{U'(q_t)\Delta}{4\pi g v(q_0, q_t)}. \qquad (17)$$

Thus, the standard semiclassical partition function is written as

$$Z = -\frac{1}{4\pi g}\sum_i \int_{q_\Theta^-}^{q_\Theta^+} dq_t \frac{U'(q_t)\Delta^{1/2}}{v(q_0, q_t)} \exp(-I[\bar{q}_c{}^i]/g), \quad (18)$$

where $v(q_0, qt) \equiv \mathrm{sign}(q_t - q_0)\sqrt{2[U(q_0) - U(q_t)]}$ and $q_\Theta^\pm \equiv \lim_{q_0 \to \pm\infty} q_t(q_0, \Theta)$. Therefore, the change of variables removes the singularity and this procedure, summing

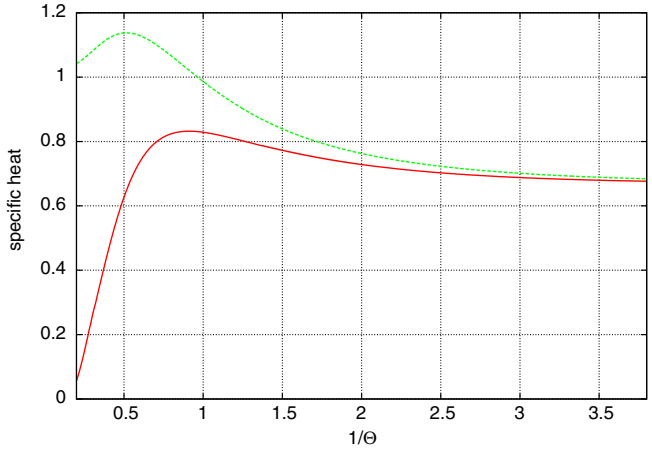

FIG. 11 (color online). Specific heat (20) vs. $1/\Theta$ for $g = 0.1$. Dashed/green: Classical result; solid/red: current approach.

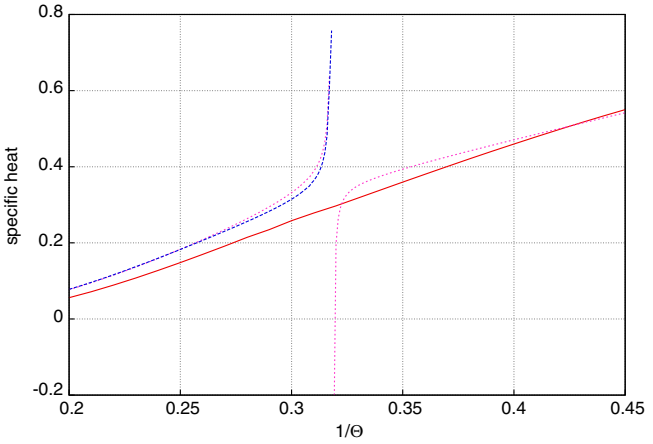

FIG. 12 (color online). Same as previous plot—specific heat (20) vs. $1/\Theta$ for $g = 0.1$—zooming in around the temperature where the first catastrophe takes place ($\Theta = \pi$). Dotted/magenta line: Only the global minimum is taken into account. Dashed/blue line: Both global and local minima are taken into account. Note that the local minimum (and therefore also this curve) exists only at low temperatures, on the left-hand side of the plot. Solid/red line: Current approach.

over the two minima of the Euclidean action, should give a reasonable approximation to the partition function.

However, thermodynamic quantities are obtained taking derivatives of the partition function and thus they are affected by the singularity. Therefore, as we are interested in computing the specific heat, we shall take our calculation up to the fourth order in the fluctuations. Notice that this is still a semiclassical expansion, for we assume that the main contribution comes from the classical solution. The calculation is depicted in Appendix B, where one can also promptly recognize the standard semiclassical expansion[5] if one stops at the second term on the right-hand side of Eq. (B8). Nevertheless, even the full expression is not useful for practical purposes, for its calculation requires the knowledge of the eigenfunction $y_0(\theta)$ and its eigenvalue c_0. There is, however, a shortcut [24]: just as in a plain fourth-order polynmial of the form [see Eq. (13) and Table I]

$$f(x) = \frac{1}{4}x^4 + \frac{a}{2}x^2 + bx + c, \tag{19}$$

the coefficients $\{a, b, c\}$ are completely determined by the values of the function $f(x)$ in 3 points. In the present case, all we need are the values of the action at the 3 extrema, easily calculated from the classical trajectories (15).

The following plots present the results obtained for the specific heat for $g = 0.1$—we argue in the next subsection that this value is small enough so that the effects of the catastrophe are relevant. In Fig. 11 we compare our results to the classical one (no quantum effects, yields correct results only at high temperatures). In Fig. 12 we zoom in around the temperature where the first catastrophe takes place (at $\Theta = \pi$) and show the results for the specific heat

$$C \equiv \Theta^2\left[\frac{1}{Z}\frac{\partial^2 Z}{\partial\Theta^2} - \left(\frac{1}{Z}\frac{\partial Z}{\partial\Theta}\right)^2\right] \tag{20}$$

from different semiclassical approaches. We plot (dotted/magenta line) the standard semiclassical approximation around the global minimum of the action, (dashed/blue line) the standard semiclassical approximation around both minima of the action, considered independent and far apart from each other (recall that there are two of them only at the left-hand, low-temperature side of the plot), and (solid/red line) the current approach. The former two calculations are supposed to diverge at the catastrophe due to the coalescence of the classical trajectories.

Here, we show the corrections that should be taken into account when the standard semiclassical approximation fails, going beyond second order in the perturbation whenever this approximation yielded divergent results. On the other hand, we still rely on the assumption that the classical solution is responsible for the main contribution to the partition function (and, consequently, to relevant thermodynamic quantities, such as the specific heat). In other words, we assume throughout the paper that the first term of the JWKB expansion of the partition function is a good approximation.

Just as in any standard quantum mechanics calculation, one does not expect the JWKB approximation to hold when the thermal energy is close to the height of the barrier, where the potential changes quickly and the classical turning points are too close to each other. Therefore, one

[5]It is also obvious then when this approximation fails: by neglecting terms of order c_0^3 and higher, Eq. (B8) yields the usual term $\Delta^{-1/2}$, which diverges at the caustic.

must require here that $E_b/E_T \equiv \Theta/(4g) \gg 1$, where $E_b \equiv V(0) - V(\pm\sqrt{mw^2/\lambda})$ is the height of the barrier and $E_T \equiv 1/\beta \equiv k_B T$ corresponds to the thermal energy. In other words, unless $g \ll \Theta_c/4 \sim 0.8$, the JWKB approximation itself will break down before the first catastrophe sets in at $\Theta_c = \pi$.

V. SUMMARY

Semiclassical approximations usually uncover important nonperturbative information about quantum systems. They are especially suited to the construction of effective theories at finite temperature, since the perturbative approach suffers from serious infrared problems and needs involved resummation techniques to provide sensible results. The boundary effective theory has proved to be very adequate to describe the thermodynamics of a thermal massless scalar theory, providing an excellent result for the pressure at leading order [19], as well as a consistent description of the thermal effective potential in the symmetric sector [20]. Its extension to the case where spontaneous symmetry breaking is present is, nevertheless, subtle, the main obstacle being the existence of multiple extrema of the action for sufficiently low temperatures and the associated bifurcations of classical solutions.

In this paper we have considered, as a toy model (however not an academic one, since the double well has, of course, applications in statistical mechanics and condensed matter physics), the analogous case in quantum statistical mechanics. We have shown how to use the tools of catastrophe theory to deal with caustics and provide finite and well-behaved results for the partition function and the specific heat. In particular, we have proved that one needs at most two relevant classical solutions in the procedure, which renders the method of practical use. As mentioned previously, this corresponds to a first step towards the study of spontaneous symmetry breaking and thermal phase transitions using the boundary effective theory, on which we plan to report soon.

ACKNOWLEDGMENTS

This work was partially supported by CAPES-COFECUB project 663/10, CNPq, FAPERJ, FAPERN, FUJB/UFRJ and ICTP. The work of E. S. F. was financially supported by the Helmholtz International Center for FAIR within the framework of the LOEWE program (Landesoffensive zur Entwicklung Wissenschaftlich-Ökonomischer Exzellenz) launched by the State of Hesse.

APPENDIX A: ELEMENTS OF CATASTROPHE THEORY

Consider a function $S(x;\nu)$ that depends on a set of coordinates $x = \{x_1, x_2, ...\}$ and certain control parameters $\nu = \{\nu_1, \nu_2, ...\}$. The number of coordinates is the dimension of the catastrophe, while the number of control parameters defines the so-called codimension of the catastrophe.

In two dimensions, S can be seen, for instance, as describing the terrain height of a certain landscape. Its maxima, minima and saddle points represent the peaks, valleys and throats. In this picture, the role of the parameters ν is to deform the topography of the landscape, changing the position of the extrema and eventually splitting or merging some of them.

The aim of catastrophe theory is to study how the pattern of the so-called generating function S is qualitatively altered when the control parameters are changed. Within this framework, one is able to understand how the extrema coalesce and separate as the parameters ν_k are varied, in a systematic and quite general approach.

Catastrophe theory [36] characterizes the stable singularities under changes in the generating functional S: those are the so-called elementary catastrophes. The splitting lemma [36] guarantees that it is always possible to write such stable generating functions in their normal forms, according to Table I. They can also be arranged hierarchically: whenever a given catastrophe is identified, all of its subordinated ones—those with the same dimension and smaller codimension—will also be present.

Let us consider the phase space (x, ν) defined by both the coordinates and control parameters of the function S. Obviously, the locus of the extrema, the so-called equilibrium surface, of S is given by

$$\frac{\partial S}{\partial x_i}(x_e, \nu) = 0, \tag{A1}$$

i.e., if for certain values of the control parameters ν, the point x_e represents an extremum of S, and the point (x_e, ν) is said to lie on the equilibrium surface.

Note, however, that no information about the nature of the extrema is given by (A1). In order to determine whether a given extremum is a minimum, maximum or a saddle point, one has to study the eigenvalues of the Hessian matrix H calculated at the equilibrium points x_e, whose elements are defined as

$$H_{ij} = \left.\frac{\partial^2 S}{\partial x_i \partial x_j}\right|_{x_e}. \tag{A2}$$

When all the eigenvalues of H are positive, we have a minimum; when all are negative, a maximum and when k are negative and the others positive, the extremum under consideration is a k saddle point.

It is clear from the previous considerations that the nature of the extrema changes when some of the related eigenvalues of H change sign. Therefore, if none of the eigenvalues is zero, a small change of the parameters will not affect the nature of the extrema.

At the bifurcation set, when one or more of the eigenvalues vanish, the situation changes drastically, as any small change of the control parameters will make the eigenvalue(s) positive or negative, changing the nature of the extremum. In other words, the qualitative aspect of the function is changed whenever the determinant of H vanishes.

One can see such behavior clearly present in Fig. 6, which represents the bifurcation set in the control parameter space, with codimension 2: crossing at the vertex corresponds to the coalescence of 3 extrema (Fig. 7): this is the cusp catastrophe. Along the bifurcation set, however, there is only one free control parameter (codimension 1)—since Eq. (14) introduces a constraint between the two of them. On this curve, only 2 trajectories coalesce (Fig. 8): this is the fold, subordinated to the cusp.

In the next Appendix, we show how one can write the action in the normal form corresponding to the cusp.

APPENDIX B: THE NORMAL FORM OF THE ACTION

In this section, we show how the action can be written in normal form, as in Eq. (13).

In the first place, we write $q(\theta) = q_{cl}(\theta) + \eta(\theta)$, so that the Euclidean action is cast in the form:

$$I[q(\theta)+\eta(\theta)] = I[q_{cl}(\theta)] + \frac{1}{2}\int_0^\Theta \eta(\theta)\left[-\frac{d^2}{d\theta^2} - 1 + 3q_{cl}^2(\theta)\right]\eta(\theta)d\theta + \int_0^\Theta \left[q_{cl}(\theta)\eta^3(\theta) + \frac{1}{4}\eta^4(\theta)\right]d\theta. \tag{B1}$$

Notice that the classical solution was not specified. There are two interesting cases: the identically null function ($q_{cl} \equiv 0$), or one of the new functions. In the latter case, the calculation is obviously made after they appear.

Now, we expand the perturbation $\eta(\theta)$ in terms of the eigenfunctions of the fluctuation operator, i.e. in terms of the functions $y_j(\theta)$ satisfying the following equation:

$$\left[-\frac{d^2}{d\theta^2} - 1 + 3q_{cl}^2(\theta)\right] y_j(\theta) = \alpha_j y_j(\theta). \tag{B2}$$

The eigenfunctions can be taken as orthonormal in the interval $[0, \Theta]$:

$$\int_0^\Theta y_i(\theta) y_j(\theta) d\theta = \delta_{ij}. \tag{B3}$$

Furthermore, they must satisfy the following boundary conditions:

$$y_j(0) = y_j(\Theta) = 0 \forall j. \tag{B4}$$

Expanding $\eta(\theta)$ in terms of $y_j(\theta)$, we have

$$\eta(\theta) = \sum_{j=0}^{\infty} c_j y_j(\theta). \tag{B5}$$

Thus, using the expansion of the fluctuations and the orthonormalization conditions, we can write the action as

$$I = I_{cl} + \frac{1}{2}\sum_j c_j^2 \alpha_j + \sum_{ijk} c_i c_j c_k \int_0^\Theta q_{cl} y_i y_j y_k d\theta + \frac{1}{4}\sum_i c_i^4. \tag{B6}$$

We have to impose the fact that the classical solution q_{cl} is an extremum of the action, therefore the fluctuations vanish, i.e. $c_j = 0$, at q_{cl}. Equivalently,

$$\left.\frac{\partial I}{\partial c_i}\right|_{c_i=0} = 0. \tag{B7}$$

This leads to the following expression for the action:

$$I \approx I_{cl} + \frac{\alpha_0}{2}c_0^2 + c_0^3 \int_0^\Theta q_{cl} y_0^3 d\theta + \frac{1}{4}c_0^4 + \sum_{j\neq 0}\frac{\alpha_j}{2}c_j^2. \tag{B8}$$

In the previous equation, $j = 0$ denotes the eigenfunction whose eigenvalue is about to vanish. Besides, we have neglected terms of the order c_j^3 for $j \neq 0$.

The difference between this expression and the usual saddle-point approximation is the inclusion of higher-order terms in the variable c_0, the one related with the vanishing eigenvalue, while only terms up to second order in the other variables, related with the other directions in functional space.

Now we perform the following change of variables:

$$z \equiv c_0 + \Upsilon \tag{B9a}$$

$$u \equiv \alpha_0 - 3\Upsilon^2 \tag{B9b}$$

$$v \equiv \Upsilon(2\Upsilon^2 - \alpha_0) \tag{B9c}$$

$$s \equiv I_{cl} + \frac{\Upsilon^2}{2}\left(\alpha_0 - \tfrac{3}{2}\Upsilon^2\right) \tag{B9d}$$

$$\Upsilon \equiv \int_0^\Theta q_{cl} y_0^3 d\theta \tag{B9e}$$

allowing us to write the action in the so called normal form, as in Eq. (13).

[1] T. Ullrich, B. Wyslouch, and J. W. Harris, Nucl. Phys. **A904–A905**, 1c (2013).
[2] M. Gell-Mann and M. Levy, Nuovo Cim. **16**, 705 (1960).
[3] B. Lee, *Chiral Dynamics* (Gordon and Breach, New York, 1972).
[4] S. P. Klevansky, Rev. Mod. Phys. **64**, 649 (1992).
[5] R. D. Pisarski, Phys. Rev. D **62**, 111501 (2000).
[6] M. Le Bellac, *Thermal Field Theory* (Cambridge University Press, Cambridge, 2000); J. I. Kapusta and C. Gale, *Finite-Temperature Field Theory: Principles and Applications* (Cambridge University Press, Cambridge, 2006).
[7] A. Mocsy, I. N. Mishustin, and P. J. Ellis, Phys. Rev. C **70**, 015204 (2004).
[8] L. F. Palhares and E. S. Fraga, Phys. Rev. D **78**, 025013 (2008).
[9] L. F. Palhares, M.Sc. thesis, Instituto de Física, Universidade Federal do Rio de Janeiro, 2008.
[10] E. S. Fraga, L. F. Palhares, and M. B. Pinto, Phys. Rev. D **79**, 065026 (2009).
[11] J. K. Boomsma and D. Boer, Phys. Rev. D **80**, 034019 (2009).
[12] A. J. Mizher, M. N. Chernodub, and E. S. Fraga, Phys. Rev. D **82**, 105016 (2010).
[13] V. Skokov, B. Friman, E. Nakano, K. Redlich, and B.-J. Schaefer, Phys. Rev. D **82**, 034029 (2010).
[14] L. F. Palhares and E. S. Fraga, Phys. Rev. D **82**, 125018 (2010).
[15] J. O. Andersen, R. Khan, and L. T. Kyllingstad, arXiv: 1102.2779.
[16] B. W. Mintz, R. Stiele, R. O. Ramos, and J. Schaffner-Bielich, Phys. Rev. D **87**, 036004 (2013).
[17] J. Berges, N. Tetradis and C. Wetterich, Phys. Rep. **363**, 223 (2002); J. M. Pawlowski, Ann. Phys. (Amsterdam) **322**, 2831 (2007); H. Gies, Lect. Notes Phys. **852**, 287 (2012).
[18] A. Bessa, F. T. Brandt, C. A. A. de Carvalho, and E. S. Fraga, Phys. Rev. D **82**, 065010 (2010).
[19] A. Bessa, F. T. Brandt, C. A. A. de Carvalho, and E. S. Fraga, Phys. Rev. D **83**, 085024 (2011).
[20] A. Bessa, C. A. A. de Carvalho, E. S. Fraga, and F. Gelis, Phys. Rev. D **83**, 125016 (2011).
[21] L. Dolan and R. Jackiw, Phys. Rev. D **9**, 3320 (1974).
[22] A. Bessa, C. A. A. de Carvalho, E. S. Fraga and F. Gelis, J. High Energy Phys. 08 (2007) 007.
[23] C. A. A. de Carvalho and R. M. Cavalcanti, Braz. J. Phys. **27**, 373 (1997).
[24] C. A. A. de Carvalho, R. M. Cavalcanti, E. S. Fraga, and S. E. Jorás, Phys. Rev. E **65**, 056112 (2002).
[25] M. C. Gutzwiller, J. Math. Phys. (N.Y.) **8**, 1979 (1967); J. Math. Phys. (N.Y.) **10**, 1004 (1969); J. Math. Phys. (N.Y.) **11**, 1791 (1970); J. Math. Phys. (N.Y.) **12**, 343 (1971).
[26] A. Lapedes and E. Mottola, Nucl. Phys. **B203**, 58 (1982).
[27] C. De Witt-Morette, A. Maheshwari, and B. Nelson, Phys. Rep. **50**, 255 (1979).
[28] B. J. Harrington, Phys. Rev. D **18**, 2982 (1978).
[29] R. P. Feynman and A. R. Hibbs, *Quantum Mechanics and Path Integrals* (McGraw-Hill, New York, 1965); R. P. Feynman, *Statistical Mechanics* (Addison-Wesley, Reading, MA, 1972).
[30] L. S. Schulman, *Techniques and Applications of Path Integration* (Dover Publications, New York, 2005)
[31] C. A. A. de Carvalho, R. M. Cavalcanti, E. S. Fraga, and S. E. Jorás, Ann. Phys. (N.Y.) **273**, 146 (1999).
[32] C. A. A. de Carvalho, R. M. Cavalcanti, E. S. Fraga, and S. E. Jorás, Phys. Rev. E **61**, 6392 (2000).
[33] L. Dolan and J. E. Kiskis, Phys. Rev. D **20**, 505 (1979).
[34] A. Cuccoli, R. Giachetti, V. Tognetti, R. Vaia, and P. Verrucchi, J. Phys. Condens. Matter **7**, 7891 (1995).
[35] M. Bachmann, H. Kleinert and A. Pelster, Phys. Rev. A **60**, 3429 (1999).
[36] P. T. Saunders, *An Introduction to Catastrophe Theory* (Cambridge University Press, Cambridge, 1980).
[37] P. F. Byrd and M. D. Friedman, *Handbook of Elliptic Integrals for Engineers and Physicists* (Springer-Verlag, Berlin, 1954).
[38] I. S. Gradhsteyn and I. M. Ryzhik, *Table of Integrals, Series, and Products* (Academic Press, New York, 2007).